Optimal Design of Flexible Imaging Modes for Agile Optical Remote Sensing Satellites

Tinghao Liu [1*], Zhen Li [1], Ting Li [1], Haitao Tang [1], Bin Liu [1], Linlu He [1] and Jing Pan [1]

[1] Institute of Remote Sensing Satellite, China Academy of Space Technology, Beijing, China
*dpimlth11@126.com

Keywords: Dynamic Imaging Modes, Agile Satellite, Optimal Design, Imaging Quality, Observation Efficiency

Abstract

By utilizing their ability to maneuver along the three axes of roll, pitch and yaw, agile satellites can point quickly at the imaging area and control the optical axis of the satellite sweep in a specific manner, thus achieve a flexible imaging work mode, which can greatly enhance the mission execution ability of the satellite, and give full play to the satellite's efficiency. Optical remote sensing satellites using dynamic imaging modes have more complex and diverse imaging modes, and the number of imaging parameters that can be combined and selected significantly increases. On the one hand, users hope that imaging quality parameters such as signal-to-noise ratio (SNR) and modulation transfer function (MTF) can meet the requirements of subsequent data applications. On the other hand, users also hope that satellite imaging efficiency can be as high as possible to meet the needs of high timeliness and rapid response of satellites. It can be seen that imaging quality and imaging efficiency are mutually constrained, and it is particularly important to strike a balance to achieve the optimal comprehensive imaging efficiency.
In this paper, a comprehensive imaging performance evaluation function and an imaging mode and parameter optimization design strategy based on this function is proposed. We hope this paper could provide valuable reference for the design of imaging mode of agile optical remote sensing satellites.

1. INTRODUCTION

1.1 Agile Optical Satellites

Satellite remote sensing technology has developed vigorously in the past half century and has made great contributions to world economic construction and scientific development. Traditional optical remote sensing satellites adopt passive push-broom mode, which means that the satellite attitude remains relatively stable and images are continuously acquired along the flight path. In recent years, high-resolution satellites have shifted towards imaging observations with higher observation efficiency, more observation angles, and more complex observation methods targeting more key areas of concern, while maintaining their passive scanning capabilities, in order to achieve refined observation.

Agile remote sensing satellites can use their ability to maneuver along the three axes of roll, pitch and yaw to quickly point to the imaging area and specifically control the optical axis of the satellite scan to achieve flexible imaging working modes, thus the mission execution capability of the satellite will be greatly improved and the efficiency of the satellite will be brought into full play.

Representative agile optical remote sensing satellites include Ikonos (Dial et al., 2003), QuickBird (Toutin and Cheng, 2002), WorldView (Anderson and Marchisio,2012), GeoEye-1 (Madden, 2009), Pleiades-1/2 (Gleyzes, et al., 2012) and the Chinese high-resolution multi-mode satellite (GFDM-1, Yu et al.,2022; Wang et al.,2021), etc. Typical flexible imaging modes of agile remote sensing satellites include co-orbital multi-point target imaging mode, co-orbital multi-strip imaging mode, co-orbital multi-angle imaging mode, co-orbital stereoscopic imaging mode, any-direction active push-broom imaging mode and other application-oriented modes (Zhang, Dai, and Liu, 2011).

1.2 Flexible Imaging Modes

1.2.1 Co-orbital Multi-point Target Imaging Mode: The satellite adjusts the camera pointing through rapid attitude maneuvers to achieve access imaging of multiple point targets scattered within the visible range of one track. This mode is designed to quickly and efficiently acquire images of multiple scattered small targets. Taking the GFDM-1 satellite as an example, the number of targets that can be obtained in one orbit is no less than 30, which is 6 times more efficient than traditional imaging satellites.

1.2.2 Co-orbital Multi-strip Imaging Mode: The satellite continuously performs multiple strip-stitching imaging of regional targets to achieve full coverage. This mode is designed to achieve rapid imaging of a large area, which can basically meet the coverage of large urban areas. If the traditional imaging method is used, multiple revisit cycles are required to complete the coverage of the corresponding area.

1.2.3 Co-orbital Multi-angle Imaging Mode: Through multiple imaging from the satellite forward to rearward vision, continuous imaging of point targets or strip targets at multiple angles can be achieved. Observation images of a specific target area at multiple different angles can be obtained. This mode can provide users with richer observation information and greatly expand the field of remote sensing applications.

1.2.4 Co-orbital stereoscopic imaging mode: The satellite achieves single-line array two-view or three-view stereo imaging through two or three imaging, and adjusts the stereo imaging base height ratio through the imaging time interval.

This mode is designed to achieve single-line array two-view or three-view stereo images. Users can specify the stereo intersection angle, or specify the observation angle for each image. This mode has flexible observation angles and can be flexibly set according to user needs to improve the level of quantitative application.

1.2.5 Any-direction active push-broom imaging mode: The satellite uses active push-broom imaging to achieve scanning imaging of a non-along-track strip target through "imaging in motion". This mode is designed to quickly acquire images of strip areas in any direction, and can image irregular long strip targets such as riverbanks, coasts, borders, roads, pipelines, etc., greatly improving the efficiency of satellite image acquisition, which can be dozens of times higher than the acquisition efficiency of traditional remote sensing satellite along-track push-broom imaging.

In addition, in this mode, the satellite's attitude maneuvers can be relied on to compensate for the impact of excessive ground speed. By using the satellite's pitch and roll maneuvers, the optical axis could have a backward compensatory speed on the ground, which is synthesized with the forward flight ground speed generated by the satellite flight. The synthetic ground speed is used for push-broom imaging, which increases the integration time, improves the signal-to-noise ratio of the remote sensing image, and reduces the requirements for the camera data rate.

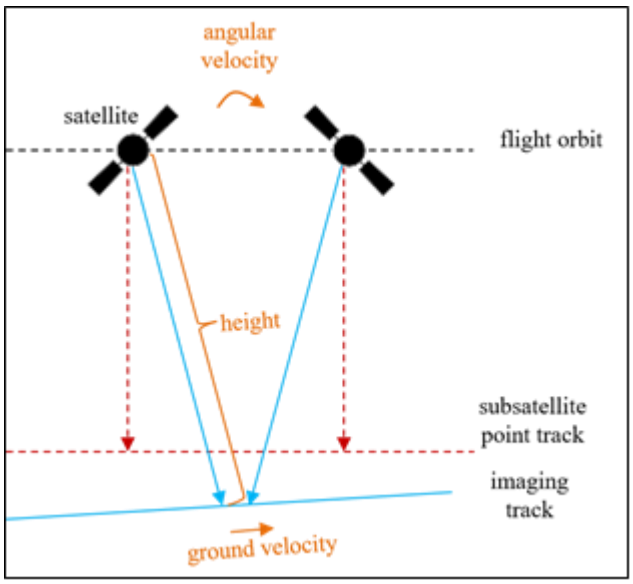

Figure 1.Schematic diagram of any-direction active push-broom imaging mode

The active push-broom imaging mode can be divided into three categories:

Uniform ground velocity mode: that is, the linear velocity of the satellite camera's visual axis pointing to the ground point on the ground surface (shown in Figure 1 as ground velocity) remains unchanged;

Uniform angular velocity mode: that is, that is, the angular velocity of the satellite camera relative to the center point of its optical axis (shown in Figure 1 as angular velocity) in the pitch direction remains unchanged;

Uniform integration time mode: also known as uniform velocity-height ratio mode, that is, the "velocity-height ratio" remains unchanged during the imaging process. The "velocity" refers to the velocity component of the projection point of the camera's visual axis pointing to the ground on the image plane (vertical optical axis) along the imaging direction (shown in Figure 1 as ground velocity). "Height" refers to the distance from the center of the camera's main mirror to the projection point of the camera's visual axis pointing to the ground (shown in Figure 1 as ‘height’). When performing attitude planning, the imaging trajectory is generally determined first, and then the "height" is determined based on the satellite position and imaging trajectory, finally the "velocity" is planned.

Generally speaking, uniform integration time mode is a more ideal active push-broomimaging mode.

2. IMPACT OF IMAGING PAREMETERS SETTING ON IMAGE QUALITY AND EFFICIENCY

For optical remote sensing satellites, dynamic MTF and signal-to-noise ratio are usually the most concerned imaging quality parameters. The integration time (that is, the retrace magnification) and the integration series are important imaging parameters that need to be set in advance when performing flexible imaging mode imaging. In this chapter, the impact of imaging parameters on imaging quality and efficiency is analyzed.

2.1 Impact on Dynamic Modulation Transfer Function (MTF)

During dynamic imaging of the satellite, the main factors affecting dynamic MTF include: camera static MTF, atmosphere, camera push-broom, integration time accuracy, drift angle correction accuracy, attitude stability, micro-vibration, space environment influence, stray light influence, defocus, etc.

The entire imaging link system can be regarded as a linear system of spatial frequency. The impact of these factors on MTF can be multiplied to determine the response of the entire system. Generally, it is necessary to quantitatively evaluate the MTF at the Nyquist frequency. The calculation relationship between the dynamic MTF of the satellite system and the MTF decrease factors of the influencing sources is as follows.

For the dynamic MTF for flight direction:

$$\begin{aligned} MTF_{flight} = & MTF_{camera} \times MTF_{atmosphere} \times MTF_{environment} \\ & \times MTF_{straylight} \times MTF_{defocus} \times MTF_{pushbroom} \\ & \times MTF_{integrationtime} \times MTF_{stability} \\ & \times MTF_{micro\text{-}vibration} \end{aligned} \quad (1)$$

For the dynamic MTF perpendicular to the flight direction:

$$\begin{aligned} MTF_{perpendicular} = & MTF_{camera} \times MTF_{atmosphere} \times MTF_{environment} \\ & \times MTF_{straylight} \times MTF_{defocus} \times MTF_{driftangle} \\ & \times MTF_{stability} \times MTF_{microvibration} \end{aligned} \quad (2)$$

The satellite dynamic MTF is as follows:

$$MTF_{satellite} = (MTF_{flight} \times MTF_{perpendicular})^{1/2} \quad (3)$$

https://doi.org/10.5194/isprs-archives-XLVIII-3-2024-305-2024

Next, the influence factors on MTF is classified according to whether it is related to the imaging parameter setting, and the influence of each factor is explained respectively.

2.1.1 Influence Factors Not Related to Imaging Parameters

Camera Static MTF： Theoretically, the static modulation transfer function of a camera should be the product of the optical system MTF, the detector MTF, and the electronic circuit MTF. In practice, it is also necessary to consider the impact of the camera manufacturing process such as optical component processing and camera assembly on the camera's static MTF.

Atmosphere: Is closely related to the time, location and atmospheric conditions of the imaging mission. Generally, under good imaging conditions on orbit, the MTF atmospheric value range of the visible light panchromatic and multi-spectral bands is 0.5~0.98.

Space Environment Influence: Due to changes in the transportation conditions of the space camera during launch (such as impact, vibration, overload, etc.) and the environmental conditions during on-orbit operation (such as pressure, temperature, microgravity, etc.), the relative positions of the primary and secondary mirrors of the optical-mechanical system will change, resulting in defocus, astigmatism and coma, leading to a decrease in image quality.

Stary Light: The non-imaging light beam from outside the view field reaches the image plane after diffuse reflection from the tube wall, which will cause uneven illumination of the detector, thereby reducing the image contrast.

$$MTF_{starylight} = \frac{1}{1+V} \tag{4}$$

where, V is the stray light coefficient.

Defocus: The effect of defocus on MTF can be evaluated using the following formula:

$$MTF_{defocus} = 2J_1(X)/X \tag{5}$$

where, J_1 is First-order Bessel function
$X=\pi d v_n$, d is the diameter of the dispersion circle caused by defocus, v_n is the spatial frequency corresponding to the Nyquist frequency.

Push-broom: For cameras that use push-broom imaging, there is an inherent drop factor in the flight direction due to push-broom:

$$MTF_{pushbroom} = \mathrm{sinc}(\pi v_n \Delta d) \tag{6}$$

where, Δd is the image displacement distance within an integration time.

Micro-Vibration: The vibrations with small amplitude and wide frequency domain that occur in the whole or part of the satellite will cause the optical camera to not image the same ground object during the imaging time, thereby causing the image quality to deteriorate:

$$MTF_{micro\text{-}vibration} = exp(-\frac{1}{2}\pi^2 (\frac{\Delta d}{d})^2) \tag{7}$$

where, Δd/d is the relative image shift within the integration time.

2.1.2 Influence Factors Related to Imaging Parameters

Integration Time: The accuracy of the integration time setting will affect the degree of synchronization between the camera TDI photogenerated charge packet transfer and the image motion on the focal plane, which in turn affects the dynamic MTF:

$$MTF_{integration\ time} = sinc(\pi v_n m c \Delta t_i) \tag{8}$$

where, m is the integration series of this imaging mission
c is the velocity of light
Δt_i is the integration time setting error.

Note that for remote sensing cameras with multiple TDICCDs, the projection size of each CCD pixel on the ground is inconsistent, which leads to inconsistent image motion speed. If the integration time of each CCD is uniformly set according to the center point integration time, the edge field of view image will cause the $MTF_{integration\ time}$ to decrease sharply due to the mismatch of image motion speed, especially after a large-angle rolling maneuver (Zhu, 2017).

Therefore, in order to ensure the MTF of the full field of view image, the satellite should use the slice setting integration time function.

Drift angle correction accuracy: During satellite imaging, the rotation of the earth causes the ground objects corresponding to each row of pixels to shift. The residual error of the drift angle correction will affect the imaging performance of the camera, mainly manifested in the image shift caused by the residual error of the correction, which causes the dynamic MTF to decrease:

$$MTF_{driftanlge} = sinc(\pi v_n m c \tan\theta) \tag{9}$$

where, θ is the residual error of drift angle correction.
Note that we can only use a certain feature point in the view field as a reference (usually the center, or the center of a certain piece of TDICCD detector) to correct the drift angle. Therefore, for other feature points, it will inevitably bring drift angle residuals.

Attitude Stability: The impact of satellite attitude stability on imaging quality is mainly reflected in the angle changes in the three directions of yaw, pitch and roll, which will cause image shift on the image plane and lead to a decrease in MTF:

$$MTF_{stablity} = sinc(m v_n T_{int} F \tan w) \tag{10}$$

where, T_{int} is the integration time
F is the focal length of the optical system
w is the attitude stability.

Summary: As can be seen from this section, when the satellite stability, integration time setting accuracy, and drift angle correction accuracy are determined, the imaging parameters that affect the dynamic MTF are mainly reflected in the integration series and integration time. In other words, if the integration

time is longer (that is, the larger the retrace imaging magnification, the slower the ground speed, and the lower the line frequency), the larger the integration series, the worse the impact on the dynamic MTF.

2.2 Impact on Signal-to-Noise Ratio (SNR)

The signal-to-noise ratio is mainly determined by the signal power and the noise power. The SNR calculation formula of the camera is (expressed in electrons):

$$SNR = \frac{n_{pe}}{n_{sys}} \tag{11}$$

where, n_{sys} is the camera system noise, which mainly includes photon shot noise, dark current noise, quantization noise, readout noise, etc.
n_{pe} is the mean value of the signal, that is, the number of electrons generated by the scene signal after photoelectric conversion on the camera detector device.

$$n_{pe} = \frac{A_{detector}\pi(1-\varepsilon)t_{\text{int}}}{4f\#^2\, hc}\int_{\lambda_{\min}}^{\lambda_{\max}} \eta(\lambda)L_{target}(\lambda)\times\tau_{optics}(\lambda)\lambda d\lambda \tag{12}$$

where, η is the quantum efficiency, that is, the average number of photoelectrons generated per incident photon, usually an indicator of the detector
τ_{optics} is the transmittance of the optical system,
ε is the optical aperture surface obstruction ratio,
$f\#$ is the F number of the optical system,
λ is wavelength, λ_{max} and λ_{min} are the upper and lower limits of the spectral passband,
t_{int} is the camera exposure time, $t_{int}=mT_{int}$
$A_{detector}$ is the area of the detector pixel,
L_{target} is the spectral amplitude brightness from the target at the camera entrance pupil,
h is Planck's constant, h=6.63×10^{-34}*Js.*

The main imaging setting parameters that affect the imaging signal-to-noise ratio are the integration time and the integration series. If the integration time is longer and the integration series is larger, the total exposure time will be longer, and the number of photons incident into the optical system will be more. To a certain extent, the imaging signal-to-noise ratio can be improved.

2.3 Impact on Observation Efficiency

The influence of imaging parameter settings on imaging efficiency is mainly reflected in that for active push-broom imaging, if the compensation factor is high (that is, longer integration time), although a higher signal-to-noise ratio can be obtained, the observation coverage within the same observation time is reduced.

Besides, under certain imaging parameter conditions (for example, each TDICCD detector is set to the same integration time, and the drift angle is corrected according to the center point), the dynamic MTF of the edge field image will be significantly reduced. For areas of the field of view where the dynamic MTF index does not meet a certain set standard, imaging in this area can be considered invalid. Thus, the effective observation coverage of this imaging mission will also be reduced.

3. AN OPTIMAL DESIGH METHOD FOR FLEXIBLE IMAGING MODES

From the analysis in the previous chapter, it can be seen that imaging quality and imaging efficiency are mutually constrained. Even obtaining the highest imaging signal-to-noise ratio and dynamic MTF is contradictory to a certain extent, since increasing the total exposure time means more incident photons and longer image shift distance at the same time. How to make a trade-off to achieve the best comprehensive imaging performance is particularly important.

In the following, a quantitative imaging comprehensive evaluation function is established by comprehensively considering the requirements of achieving high imaging quality parameters and high imaging efficiency. Based on this evaluation function, imaging parameters could be selected to achieve the optimal comprehensive performance. After the introduction, a specific imaging mission in a hypothetical application is chosen as an example.

3.1 Comprehensive Evaluation Function Definition and Composition

The comprehensive evaluation function g is defined as

$$g = (ma + nb + pc)\times 100 \tag{13}$$

where, a is the evaluation value of the imaging quality parameter $\{A\}$,
b is the evaluation value of the imaging efficiency parameter B,
c is the evaluation value of the ratio of detectors that meet the dynamic MTF standard MTF_0.
m, n, and p are weight coefficients assigned according to the importance of the indicators, and m+n+p=1.

The evaluation value a of imaging quality parameter $\{A\}$ is further decomposed into:

$$a = \sum x_i a_i \tag{14}$$

where, a_i is the evaluation value of the imaging quality parameter A_i, that is, the ratio of the actual imaging parameter to the evaluation benchmark parameter
x_i is the corresponding weight coefficient, $\sum x_i = 1$.

a_i can be further decomposed according to the actual satellite imaging spectrum. For example, A_1 corresponds to the dynamic MTF index, which can be further decomposed into the MTF of multiple spectrums such as visible light panchromatic and multispectral. A_2 represents the signal-to-noise ratio index, which can also be decomposed according to the spectrum segment.

The evaluation value b of the imaging efficiency parameter B can be expressed as:

$$b = \frac{L}{T_L v_0} \tag{15}$$

where, L is the length of the imaging strip,
T_L is the length of the entire process from the satellite's attitude adjustment to the start of imaging to the attitude returning to the subsatellite point

v_0 is the maximum ground velocity of the satellite, that is, the ground scanning speed of the satellite when no attitude maneuvers are performed. For high-orbit optical satellites, v_0 can be set to the satellite's typical ground scanning speed or the satellite's maximum capability of ground scanning velocity.

The evaluation value c represents the ratio of the number of detectors whose dynamic MTF is better than the set threshold MTF_0 to the total number of detectors.

3.2 A Specific Imaging Mission Example

Below, taking a hypothetical agile optical remote sensing satellite with the ability of flexible imaging modes as an example, the optimal design method is explained in detail.

3.2.1 Input for this imaging mission: A hypothetical agile optical remote sensing plans to observe the target at 9:00 UTC on March 20, 2025. The strip length is 20km. The solar altitude angle at the imaging time is calculated to be 30 degrees, and the surface reflectivity is 0.2.

3.2.2 Select the satellite imaging mode: According to the actual capabilities of this hypothetical satellite, select the uniform integration time plan for subsequent imaging parameter design.

3.2.3 Setting weight coefficients and evaluation benchmark parameters: according to the actual requirements of imaging quality and imaging efficiency of this mission, the weight coefficients m, n and p are assigned to 0.6, 0.3 and 0.1. Thus, $g=0.6a+0.3b+0.1c$ in this case.

In this example, the evaluation value a is decomposed into: $a=0.6a_1+0.4a_2$, where a_1 represents the dynamic MTF evaluation value, and a_2 represents the signal-to-noise ratio evaluation value. This mission only involves imaging the entire visible and near-infrared spectrum, so a and b are not further decomposed.

A total of 18 detectors are involved in the imaging task, and the maximum ground velocity of the satellite v_0 is 7 km/s.

The dynamic MTF benchmark MTF_0 is set as 0.1 (in the entire field of view) and the SNR benchmark SNR_0 is set as better than 40dB.

3.2.4 Establish possible set of imaging parameter selections: Including retrace imaging magnification and integration series. The possible imaging parameter selection set for hypothetical satellite includes: retrace imaging magnification {1,2,5,10}, and integration series {24,48,96}.

3.2.5 Score a combination of imaging parameters: Select an imaging parameter combination, retrace imaging magnification as 2, and the integration series as 24, we start to perform orbit calculation and attitude planning. Then using the center point of detection field as the reference, the drift angle correction is performed, and the imaging quality (MTF and SNR) is calculated.

After calculation, the MTF values of detectors 1 and 18 do not meet the benchmark MTF_0, so they are removed and $c=16/18=0.89$

After removing the substandard detectors, the average MTF in the field of view is 0.11. Thus $a_1=0.11/0.1=1.1$. The signal-to-noise ratio is 32dB, so $a_2=32/40=0.8$.

Therefore, the imaging quality evaluation value $a=0.6\times1.1+0.4\times0.8=0.98$.

The length of the imaging strip is L=20km, the total time length of the satellite from attitude adjustment to imaging to attitude return to the subsatellite point is T=24s, and the maximum ground speed of the satellite is v_0=7km/s, so b=0.12.

Therefore, the imaging comprehensive evaluation value g is calculated as 71.3 points for this combination of imaging parameters:

3.2.6 Best parameter combination selection: After traversing various imaging parameter combinations, the combination with the highest comprehensive evaluation value g was selected: retrace imaging magnification as 4, and the integration series as 48. At this time, a=1.21, b=0.09, c=0.83, and the comprehensive evaluation value g=83.6.

3.2.7 Note: The above calculation process can be performed on the ground and then uploaded to the satellite for execution. Alternatively, if the satellite's onboard computer has the capability, it can perform orbit extrapolation and attitude planning based on the uploaded mission parameters and select the optimal parameter combination for execution.

The above is only an example for a hypothetical satellite. The weights of various evaluation factors can be set specifically according to different imaging mission. Satellite designers and users can also revise the items and weights of the evaluation function according to their own needs. For example, for infrared detection satellites, sensitivity can be used as an important evaluation indicator.

4. SUMMARY

The flexible imaging mode of agile satellites can greatly improve the satellite's observation capability and image quality. However, how to achieve the best comprehensive imaging is a difficult problem to decide when setting imaging parameters. This paper proposes an optimization design method for the flexible imaging mode of agile optical satellites. Through this method, the best comprehensive imaging solution can be selected for satellite execution among various imaging requirements that constrain each other.

Acknowledgement

The authors would like to express their gratitude to Dr. Qiang Yu, Dr. Shaocong Liu, Dr. Xianfei Qiu, Mr. Zixi Guo and Prof. Jianbing Zhu for helpful discussion.

References

Dial, G., Bowen, H., Gerlach, F., Grodecki, J., and Oleszczuk, R. (2003). IKONOS satellite, imagery, and products. *Remote sensing of Environment*, 88(1-2), 23-36.

Toutin, T., and Cheng, P. (2002). QuickBird – a milestone for high resolution mapping. *Earth Observation Magazine*, 11(4), 14-18.

Anderson, N. T., and Marchisio, G. B. (2012). WorldView-2 and the evolution of the DigitalGlobe remote sensing satellite constellation: introductory paper for the special session on WorldView-2. *Algorithms and Technologies for Multispectral, Hyperspectral, and Ultraspectral Imagery XVIII* (Vol. 8390, pp. 166-180). SPIE.

Madden, M. (2009). GeoEye-1, the world’s highest resolution commercial satellite. *International Quantum Electronics Conference* (p. PWB4). Optica Publishing Group.

Gleyzes, M. A., Perret, L., and Kubik, P. (2012). Pleiades system architecture and main performances. The International Archives of the Photogrammetry, *Remote Sensing and Spatial Information Sciences*, 39, 537-542.

Yu, J., Liang, X., Liang, D., and Yu, L. (2022). Quality Assurance and Verification of GFDM Satellite Imagery. *Chinese Conference on Image and Graphics Technologies* (pp. 55-68). Singapore: Springer Nature Singapore.

Wang, Y., Fan, L., and Li, Y.(2021) Research and Application of Agile Remote Sensing Technologies in GFDM-1 Satellite. *Spacecraft Engineering*, 30(3), 27-35 (in Chinese).

Zhang, X., Dai, J., Liu F. (2011) Research on working mode of remote sensing satellite with agile attitude control. *Spacecraft Engineering*, 20(4), 32-38 (in Chinese).

Zhu, J., Zhang, M., Wang L., Yuan, L. Cheng, B., Zhao, W.(2017). An integral time calculation method for agile satellite. *Chinese Space Science and Technology*, 37(1), 97-103(in Chinese).